

Antibacterial Optimization of 4-Aminothiazolyl Analogues of the Natural Product GE2270 A: Identification of the Cycloalkylcarboxylic Acids

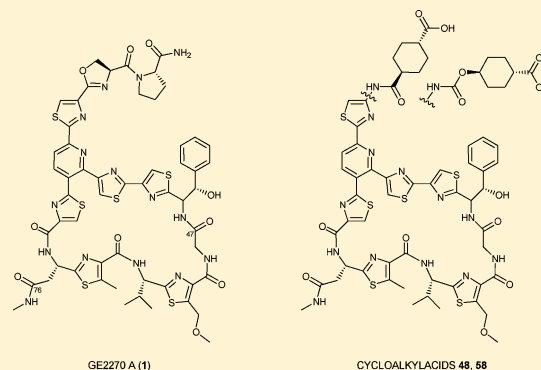
Matthew J. LaMarche,^{*,†} Jennifer A. Leeds,[‡] Kerri Amaral,[‡] Jason T. Brewer,[†] Simon M. Bushell,[†] Janetta M. Dewhurst,[†] JoAnne Dzink-Fox,[‡] Eric Gangl,[†] Julie Goldovitz,[‡] Akash Jain,^{||} Steve Mullin,[‡] Georg Neckermann,[‡] Colin Osborne,[‡] Deborah Palestrant,[§] Michael A. Patane,[†] Elin M. Rann,[†] Meena Sachdeva,[‡] Jian Shao,[†] Stacey Tiamfook,[‡] Lewis Whitehead,[†] and Donghui Yu[‡]

[†]Global Discovery Chemistry, [‡]Infectious Disease Area, and [§]Protein Structure Group, Novartis Institutes for Biomedical Research, Cambridge, Massachusetts 02139, United States

^{||}Chemical and Pharmaceutical Profiling, Novartis Pharmaceuticals, Cambridge, Massachusetts 02139, United States

S Supporting Information

ABSTRACT: 4-Aminothiazolyl analogues of the antibiotic natural product GE2270 A (**1**) were designed, synthesized, and optimized for their activity against Gram positive bacterial infections. Optimization efforts focused on improving the physicochemical properties (e.g., aqueous solubility and chemical stability) of the 4-aminothiazolyl natural product template while improving the in vitro and in vivo antibacterial activity. Structure–activity relationships were defined, and the solubility and efficacy profiles were improved over those of previous analogues and **1**. These studies identified novel, potent, soluble, and efficacious elongation factor-Tu inhibitors, which bear cycloalkylcarboxylic acid side chains, and culminated in the selection of development candidates amide **48** and urethane **58**.



INTRODUCTION

Clinical resistance to marketed drugs is becoming increasingly common.¹ Therefore, the discovery of antibiotics that act via novel mechanisms of action remains a pressing unmet medical need in infectious disease care. In particular, treating Gram positive skin and soft tissue infections caused by methicillin resistant *S. aureus*, vancomycin resistant enterococci, and group A streptococci remain distinct clinical challenges. In 1991, Selve and co-workers from Lepetit Research Institute reported the structure and antibiotic activity of GE2270 A (**1**, Figure 1). This thiopeptide-based natural product was isolated from a fermentation broth of *Planobispora rosea* and found to inhibit the prokaryotic chaperone elongation factor Tu (EF-Tu).² The in vitro antibiotic profile against methicillin resistant staphylococci, vancomycin resistant enterococci, and group A streptococci was exquisite, with minimum inhibitory concentrations below 1 $\mu\text{g}/\text{mL}$.

Previously, we described lead finding activities associated with **1** concerning the identification, decomposition, and subsequent stabilization of 4-aminothiazolyl analogues.³ Because of promising initial in vitro results, the 4-aminothiazolyl template was selected for further medicinal chemistry optimization. Specifically, a substantial increase in aqueous

solubility would be necessary in order to formulate the compounds for infused intravenous drug delivery, as the aqueous solubility of **1** was undetectable in our assays (detection limit, 5 ng/mL). The improved aqueous solubility and formulability would allow for in vivo efficacy evaluation in murine infection models (vide infra), an important preclinical milestone for this novel antibacterial chemical template, and also allow for comparison to the standards of care for soft tissue infections (i.e., linezolid, daptomycin).

As part of the strategy to further chemically stabilize the 4-aminothiazole macrocyclic appendage while increasing intrinsic aqueous solubility and improving cellular antibacterial activity, a variety of linkers, spacers, and termini were examined (Tables 1–5). Four organisms comprised our antibiotic activity characterization efforts: *Enterococcus faecalis*, *Enterococcus faecium*, *Staphylococcus aureus*, and *Streptococcus pyogenes*.⁴ In addition, the antibacterial activity of all analogues against *Streptococcus pneumoniae* (not shown) did not differ significantly compared to *Streptococcus pyogenes*. In order to confirm that the novel analogues were acting via inhibition of EF-Tu, all

Received: July 14, 2011

Published: October 14, 2011

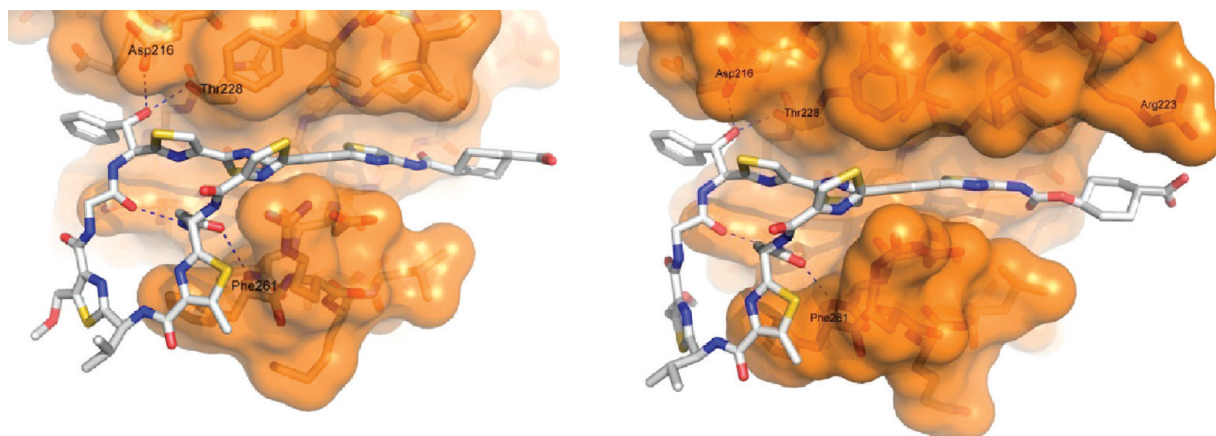


Figure 1. Cocrystal structures: *E. coli* EF-Tu and 48 (left) and 58 (right).

Table 1. Structure–Activity Relationships of the Linker Region

Linker–Spacer–Terminus	Compound	MIC assay: $\mu\text{g/mL}$				
		<i>E. faecalis</i>	<i>E. faecium</i>	<i>S. aureus</i>	<i>S. pyogenes</i>	G258D mut.
	(1)	0.5	0.25	0.25	1	
	(7)	1	1	2	>32	>32
	(8)	2	4	2	>32	>32
	(9)	4	>32	4	>32	>32
	(3)	>128	>128	>128	>128	>32
	(10)	2	4	4	>32	>32
	(11)	1	2	1	8	>32

compounds (Tables 1–5) were monitored for antibacterial activity against a 1-resistant mutant of *S. aureus* with a nucleotide change in the *tufA* gene (encoding EF-Tu). The mutation conferred a single amino acid substitution (G258D) in the thiopeptide binding pocket of the protein.⁵

RESULTS

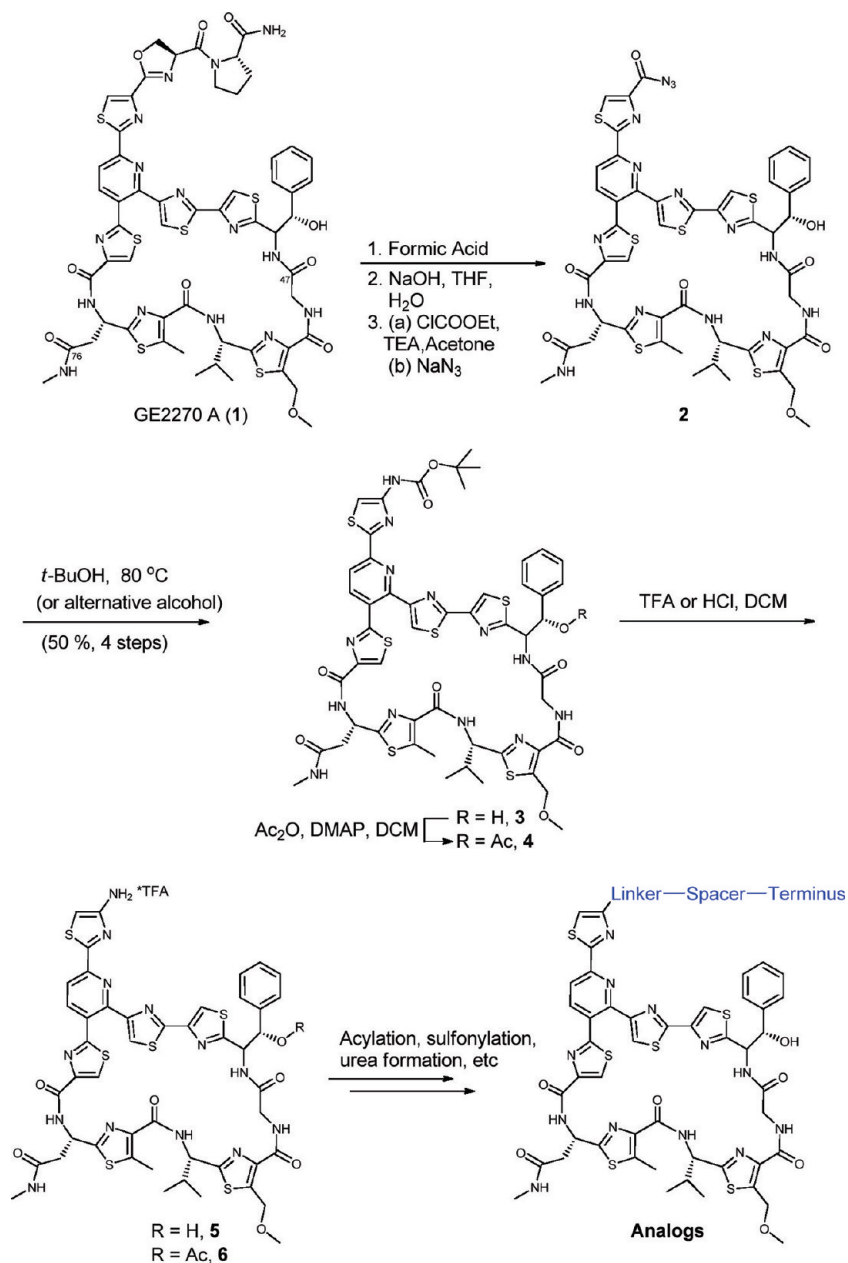
1 (Scheme 1) was first subjected to acid-catalyzed rearrangement and basic hydrolysis,⁶ which afforded the acid in high yield (quant.). The resulting 4-thiazolylcarboxylic acid was next activated with ethyl chloroformate to form the ethyl acylcarbonate, which was displaced in situ by azide. This three-step, one-pot process (50% yield) furnished the acylazide and also set the stage for the Curtius rearrangement. Alternatively, direct acylazide formation from the carboxylate utilizing diethylphosphorylazide led to variable, unreproducible yields. The acylazide was heated in *tert*-butyl alcohol (80 °C) or other alcohols (vide infra). Subsequent deprotection under acidic conditions (TFA or HCl in DCM) afforded 4-aminothiazole 5. Unfortunately basic workup, chromatography, or storage of the 4-aminothiazole free base proved difficult, as hygroscopicity ultimately led to chemical decomposition.³

However, functionalizing the amine via acylation, sulfonylation, urea formation, or imidazole formation stabilized the 4-aminothiazole. This approach enabled the design, synthesis, and biological evaluation of analogues that varied at the 4-aminothiazolyl side chain in three respects: the linker, the terminus, and the spacing between the linker and the terminus (Scheme 1).

During the initial optimization phase, a variety of linkers were evaluated for chemical stability and antibacterial activity. Amide, urethane, imidazole, sulfonamide, and urea linkers all stabilized the 4-aminothiazole (Table 1),⁷ but the antibacterial activity was variable. Compounds 7–11 displayed moderate to weak activity (MIC of 1 to >32 $\mu\text{g/mL}$). Universally, compounds 7–11 were weakly active against *S. pyogenes*. Compound 11 maintained the highest and broadest spectrum of activity. The structurally related boc-protected aminothiazole was inactive (MIC for 3, >128).

Analogues with varying termini were next designed, synthesized, and evaluated for antibacterial activity (Table 2). Nonpolar termini such as trifluoromethyl, carboxy ester, carboxamide, and PEGylated functional groups (compounds 13–16) maintained moderate (>1–4 $\mu\text{g/mL}$) to good (<1 $\mu\text{g/}$

Scheme 1. Synthesis of 4-Aminothiazolyl Analogues



mL) MICs, although without activity against *S. pyogenes* (MIC > 32 µg/mL) and mixed results against *S. aureus* (MIC of 0.5 to >32 µg/mL). By use of an in vitro bacterial cell extract assay measuring inhibition of protein synthesis in the absence of the cell membrane, these nonionizable molecules gave mixed results (2.4 to >32 µM).⁸ This was presumed to be the result of poor solubility of the compounds lacking ionizable functional groups (vide infra). Therefore, analogues substituted with more polar termini were explored: hydroxyl, amino, carboxylic acid, and phosphoric acid functionalities (compounds 17–21). Hydroxyl and amino functional groups maintained moderate antibacterial activity (MICs for 17–19, 0.5–4 µg/mL), including against *S. pyogenes*. The carboxylic acid containing analogue (20) displayed the most potent protein synthesis inhibition (IC₅₀ = 1.2 µM) in cell extracts and antibacterial activity (MIC of 0.06–4 µg/mL). Carboxylic acid 20 was studied in a mouse sepsis model of infection⁹ and displayed

potent antibacterial activity against *S. aureus* and *E. faecalis* sepsis models (ED₅₀ of 10.5 and 5.5 mg/kg, respectively). The carboxylate functional group proved useful for in situ salt formation during formulation.¹⁰ Incorporating the more polar phosphoric acid terminal group eliminated antibacterial activity altogether (21, MIC > 32 µg/mL); however, 21 inhibited protein synthesis in cell extracts (IC₅₀ = 1.5 µM). Therefore, the observed MIC values for 21 may be due to poor cellular penetration related to the polarity of the phosphoric acid moiety. In summary, a range of termini functional groups including nonpolar, hydroxyl, amino, and acid moieties displayed moderate to excellent antibacterial activity in vitro, and carboxylate 20 displayed encouraging antibacterial activity in vivo.

These results (Table 2) prompted further evaluation of two additional series of derivatives, amines (Table 3) and carboxylic acids (Tables 4 and 5). Alternative functional groups to

Table 2. Structure–Activity Relationships of the Terminus

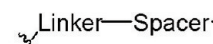
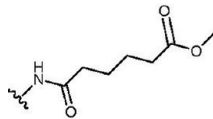

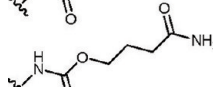
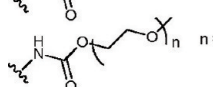
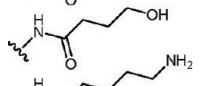
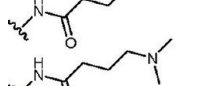
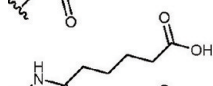
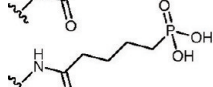


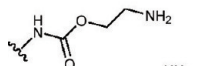
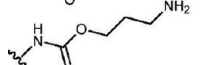
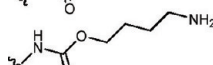
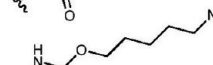
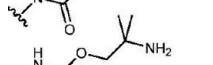
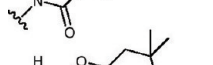

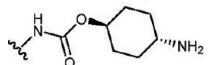
Linker—Spacer—Terminus 	Compound	Extract IC ₅₀ (μM)	MIC assays: μg/mL				ED ₅₀ (mg/kg) Staph, Ent
			<i>E. faecalis</i>	<i>E. faecium</i>	<i>S. aureus</i>	<i>S. pyogenes</i>	
	(13)	>32	4	2	>32	>32	
	(14)	>32	1	1	>32	>32	
	(15)	2.4	0.25	0.25	0.5	>32	
	(16)	10.8	0.5	0.5	4	>32	
	(17)	>16	0.5	0.5	1	>32	
	(18)	1.9	0.5	1	1	4	
	(19)	2.6	0.5	1	1	4	
	(20)	1.2	0.06	0.125	0.125	4	10.6, 5.5
	(21)	1.5	>32	>32	>32	>32	


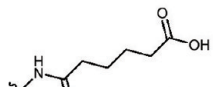
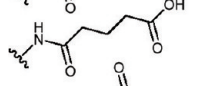
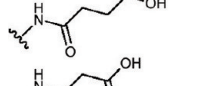
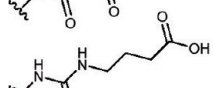
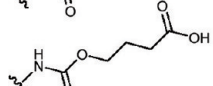
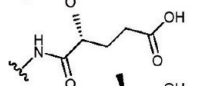
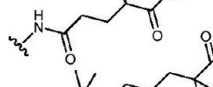
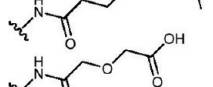
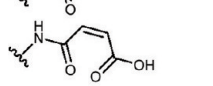
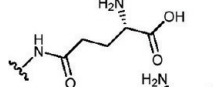
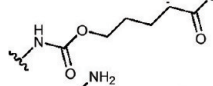
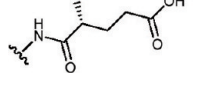
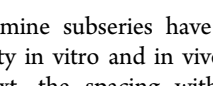
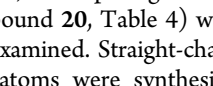
Table 3. Structure–Activity Relationships of the Spacer Region (Amines)

Linker—Spacer—Terminus 	Compound	MIC assays: μg/mL				ED ₅₀ (mg/kg) <i>S. aureus</i> , <i>E. faecalis</i>
		<i>E. faecalis</i>	<i>E. faecium</i>	<i>S. aureus</i>	<i>S. pyogenes</i>	
	(22)	1	1	1	16	
	(23)	1	1	1	16	
	(24)	0.5	1	1	8	6.48, ND
	(25)	0.5	0.5	1	8	
	(26)	1	1	2	8	
	(27)	1	0.5	1	8	
	(28)	0.5	0.5	1	8	19.3, <3.3
	(29)	0.5	0.5	1	>32	

examine the spacing between the linker and terminus were designed, synthesized, and evaluated for antibacterial activity *in vitro* and *in vivo*. The functional groups selected included acyclic, branched acyclic, carbocyclic, heterocyclic, heteroacyclic, aromatic, and heteroaromatic groups. In the amine subseries (Table 3), varying the spacing length from three to six atoms (urethanes **22**–**25**), branching of the spacing moiety (**26**–**28**), and the tertiary amine **29** proved inconsequential

(MIC of 0.5 to >32 μg/mL). Furthermore, all of the amines consistently inhibited prokaryotic protein synthesis in cell extracts as before (IC₅₀ of 0.9–3.4 μM, data not shown) and displayed no antibacterial effect on the 1-resistant mutant of *S. aureus* (data not shown). Two amines (**24** and **28**) were studied in a mouse sepsis model of infection and displayed *in vivo* activity (ED₅₀ of 3.3–19.3 mg/kg), albeit variable. Apparently, the spacing length and substitution pattern within

Table 4. Structure–Activity Relationships of the Spacer Region (Acyclic Acids)

Linker–Spacer–Terminus 	Compound	MIC assay: $\mu\text{g/mL}$				ED ₅₀ (mg/kg) <i>S. aureus</i> , <i>E. faecalis</i>
		<i>E. faecalis</i>	<i>E. faecium</i>	<i>S. aureus</i>	<i>S. pyogenes</i>	
	(20)	0.06	0.125	0.125	4	10.6, 5.5
	(30)	0.25	0.5	0.25	8	
	(31)	0.25	0.5	0.25	4	
	(32)	1	2	1	8	
	(33)	1	4	1	16	
	(34)	0.03	0.06	0.06	1	5.4, 3.1
	(35)	0.25	0.5	0.25	4	10.6, 11.1
	(36)	0.125	0.25	0.25	4	
	(37)	1	1	4	>32	
	(38)	0.5	2	0.5	4	
	(39)	1	2	1	16	
	(40)	>32	>32	>32	>32	
	(41)	8	32	8	8	
	(42)	0.5	1	1	>32	9.5, >60

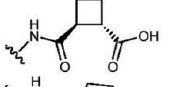
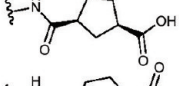
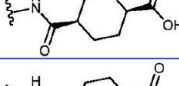
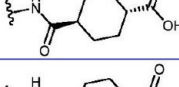
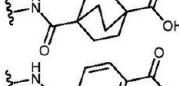
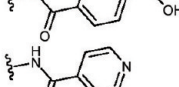
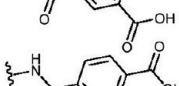
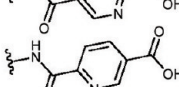
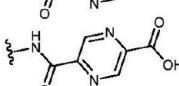
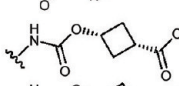
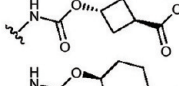
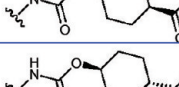
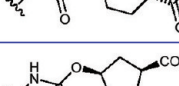
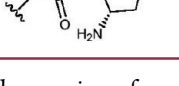
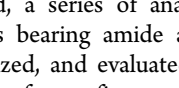
the amine subseries have little or no effect on antibacterial activity in vitro and in vivo.

Next, the spacing within the carboxylate subseries (e.g., compound 20, Table 4) was explored. First, the spacing length was examined. Straight-chain alkyl spacers ranging from one to four atoms were synthesized and evaluated for antibacterial activity; the four atom analogue (e.g., 20) between the amide and the carboxylate terminus (totaling eight atoms for the entire side chain) proved superior in MIC assays. Longer spacing lengths failed to provide any advantage (data not shown). In addition, urethanes and ureas were revisited using the optimized linker-spacing–termini length of eight atoms; urethane 34 emerged as one of the most potent derivatives within the 4-aminothiazole class. Further studies included methyl and gem-dimethyl substituents on the linker (35–37); these analogues retained moderate to potent antibacterial activity, respectively (MICs for 35 and 36, 0.25–4 $\mu\text{g/mL}$; MIC for 37, 1 to >32 $\mu\text{g/mL}$). More conformationally restricted functional groups, which included a heteroatom and

a cis-olefin, also retained moderate activity (MIC for 38, 0.5–4 $\mu\text{g/mL}$; MIC for 39, 1–16 $\mu\text{g/mL}$). Incorporating a second ionizable group, for example, an amine (40–42), provided varying results. The activity appeared sensitive to the location of the amino group on the spacer and its proximity to the carboxylate moiety. Placing the amino group further from the terminal acid proved superior, which is supported by comparing 42 (MIC of 0.5 to >32 $\mu\text{g/mL}$) to α -amino acids 40 and 41 (MIC of 8 to >32 $\mu\text{g/mL}$). Importantly, all carboxylates in Table 4 inhibited protein synthesis in cell extracts (IC₅₀ of 1.2–7.8 μM) but displayed no antibacterial effect on the 1-resistant mutant of *S. aureus* (data not shown). Importantly, in the mouse sepsis infection model, the most potent carboxylates (20, 34, 35, and 42) and urethane 34 demonstrated potent antibiotic activity, which is consistent with the in vitro results.

Since the carboxylate analogues containing conformational restrictions (e.g., 35–39) retained antibacterial activity, we decided to further probe structure–activity relationships utilizing carbocyclic and aromatic functional groups. Toward

Table 5. Structure–Activity Relationships of the Spacer Region (Cyclic Acids)

Linker–Spacer–Terminus	Compound	MIC assays: $\mu\text{g/mL}$				ED ₅₀ (mg/kg)
		<i>E. faecalis</i>	<i>E. faecium</i>	<i>S. aureus</i>	<i>S. pyogenes</i>	<i>S. aureus</i> , <i>E. faecalis</i>
	(45)	0.25	0.5	0.25	4	
	(46)	0.25	0.25	0.25	4	
	(47)	0.125	0.25	0.25	4	
	(48)	0.06	0.06	0.125	4	5.2, 0.6
	(49)	0.125	0.25	0.25	4	
	(50)	0.125	0.125	0.125	4	
	(51)	2	8	8	>32	
	(52)	4	8	4	>32	
	(53)	0.125	<0.06	0.25	4	4.4, 0.8
	(54)	0.25	0.25	0.5	8	13.9, 2.2
	(55)	0.06	0.03	0.06	1	2.9, 1.0
	(56)	0.06	0.06	0.125	2	
	(57)	0.125	0.125	0.125	1	
	(58)	0.06	0.03	0.125	2	4.3, 0.2
	(59)	1	4	2	2	

this end, a series of analogues with different cyclic spacing moieties bearing amide and urethane linkers were designed, synthesized, and evaluated for antibacterial activity (Table 5). Multiple four-, five-, and six-membered carbocyclic-linked amides were investigated along with their stereochemical isomers and bridged congeners, and many retained very potent antibacterial activity (MICs for 45–49, 0.06–4 $\mu\text{g/mL}$). The trans-cyclohexylamide analogue (48) provided the best antibacterial profile of the carbocyclic-linked amides, with MICs in the 0.06–4 $\mu\text{g/mL}$ range. In addition to the saturated cycloalkyl congeners, aromatic functional groups (50–54) were evaluated. The phenyl linked analogue retained potent antibacterial activity (50, 0.125–4 $\mu\text{g/mL}$), while heteroaromatic groups (51–54) produced mixed results; the location of the nitrogen atom appeared to play a role in the SAR. This observation is consistent with previous findings within the acyclic subseries (Table 4). Pyridine-based analogues with an ortho-acid in both 1,4 and 1,3 acid–amide systems diminished

the antibacterial activity (51 and 52, 2 to >32 $\mu\text{g/mL}$), while the meta-acid retained potent antibacterial activity (53, 0.06–4 $\mu\text{g/mL}$). Within the urethane subseries (55–59), similar cycloalkyl groups (cis/trans cyclobutyl and cycloalkyl) were profiled and produced results similar to those of the amide series, albeit with modestly improved MIC activity (56–58, 0.03–2 $\mu\text{g/mL}$). Subsequent addition of an amino substituent conferred a loss of antibacterial activity (59, 1–4 $\mu\text{g/mL}$). Importantly, all carboxylates in Table 5 inhibited protein synthesis in cell extracts and also displayed no antibacterial effect against the 1-resistant mutant of *S. aureus* (not shown). In vivo studies in a mouse sepsis model confirmed the antibiotic activity of the most potent carboxylates (48, 53, 54, 55, and 58). Interestingly, amide 48 and urethane 58 exhibited exquisite in vivo effects (e.g., enterococci ED₅₀ < 1 mg/kg), which was consistent with their excellent potency in vitro and warranted additional characterization (vide infra).

Several compounds from these lead optimization studies were examined in cocrystallographic studies with EF-Tu derived from *Escherichia coli*, including amide **48** and urethane **58**.¹⁰ A number of cocrystal structures were solved with varying linkers, spacers, and termini. The cocrystal structures of amide **48** and urethane **58** (Figure 1) confirmed that the analogues bind within domain 2 of EF-Tu and revealed that the macrocyclic conformations of **48** and **58** resemble **1** in its bound conformation.¹¹ Additionally, similar interactions were observed between **48/58** and EF-Tu compared to **1** including H-bonding with EF-Tu at several locations (Thr228, Asp216, Asn273, Phe261). Intramolecular H-bonding across the macrocycle from the secondary amide (donor) to the glycine carbonyl (acceptor) was also observed, which may contribute to conformational stabilization. In the aminothiazolyl region, the amide linker (**48**) and the urethane linker (**58**) both orient the cyclohexylcarboxylic acid side chain toward solvent as well as Arg223. We speculate that both the cyclohexane functional motif and the appropriate linker–terminus spacing orients the carboxylate favorably for interaction with Arg223. Further exploitation of this interaction will be the subject of future communications.

In order to further characterize **48** and **58** in vivo, we next embarked on comprehensive solubility and formulation studies. The solubilities of **48** and **58** were first analyzed at various pH values (Table 6). This revealed a pH dependency (as expected

Table 6. Solubility Data for 48 and 58^a

vehicle	48	58
pH		
pH 1.0	BLD (1.1)	BLD (1.1)
pH 4.63	BLD (4.7)	BLD (4.7)
pH 7.4	0.3 (7.3)	0.001 (7.4)
pH 12.0	2.441 (9.3)	2.0 (10.7)
cosolvent		
ethanol	6.7	9.6
PEG400	>15.7	>7.6
PG	>14.8	>7.4
surfactant		
10% Cremophor	1.5	1.1
1% Pluronic F-68	0.9	BLD
20% Solutol HS 15	2.6	1.7
1% Tween 80	0.9	0.3
10% VitE TPGS	1.9	3.0
counterion		
0.1 M NH ₄ OH	8.9	3.0
0.1 M L-arginine	4.7	3.0
0.1 M glutamine	9.5	2.0
0.1 M lysine	9.5	1.8
0.1 M KOH	4.1	1.9
0.1 M NaOH	5.7	1.0

^aSolubility in mg/mL. Values in parentheses indicate the final pH. BLD = below limit of detection.

for carboxylic acid-containing compounds) where solubility in buffer increased at higher pH. For example, at low pH (1–4), the solubility was below the limit of detection, while at higher pH (7–10) the solubility increased to the mg/mL range. We

also evaluated cosolvents and found that alcoholic and PEG based cosolvents delivered formulations with concentrations exceeding 5 mg/mL. In addition, a variety of surfactants were screened (e.g., Cremophor, Solutol, and VitE TPGS) and increased solubility. Considering the nature of the carboxylic acid functional group, counterions were also screened, and as expected, a variety of basic modulators (i.e., NaOH, NH₄OH, lysine, etc.) increased solubility via in situ salt formation. Taken together, the final formulation for both **48** and **58** achieved up to 20 mg/mL with >1 week solution stability and consisted of 15% v/v NaOH (0.1 N), 5% v/v PEG-300, 25% saline (0.9%), 55% v/v water for injection with a final pH of 7.2–7.8. Thus, the carboxylic acid moiety proved crucial in identifying a developable formulation suitable for intravenous infusion because of its ability to form in situ salts with counterions.

Next, we evaluated the pharmacokinetics of **48** in male Sprague–Dawley rats (Figure 2). Three doses were adminis-

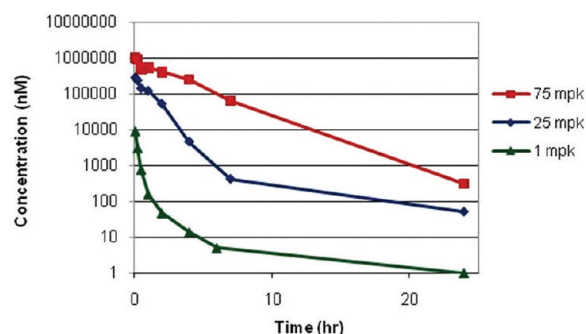


Figure 2. Pharmacokinetic data for **48** at 1, 25, and 75 mg/kg in Sprague–Dawley rats (iv bolus).

tered via iv (bolus) at 1, 25, and 75 mg/kg (Figure 1). High C_{max} (5 μ M, 320 μ M, and >1 mM, respectively) and AUC (3, 343, and 2864 μ M·h, respectively) were achieved, while Vd_{ss} (<0.1 L/kg, all doses) and CL (6.7, 1.0, 0.4 mL min⁻¹ kg⁻¹, respectively) were consistently low. High plasma protein binding was observed for both compounds (>99%). We speculate that the decrease in CL at higher doses was due to saturation of clearance mechanisms. Most noteworthy was the nonlinearity observed in overall exposure (AUC/dose: 3, 13.7, 38.2 μ M·h/mg/kg, respectively). The pharmacokinetics of **58** did not differ significantly (data not shown). In addition, other experiments assessed the oral bioavailability of the compounds, which proved very low ($F < 0.1\%$).

Because of the excellent in vitro profile, solubility, and efficacy in the sepsis model of infection, **48** was subsequently profiled in the neutropenic thigh infection model (Figure 3).¹² In this experiment, animals were pretreated with cyclophosphamide to induce neutropenia, infected with *S. aureus* (1×10^6 cfu/mouse) in the left thigh, then treated 2 h after infection with **48** or positive control (daptomycin, linezolid). After 12 or 24 h the thighs were excised, homogenized, and evaluated for bacterial colony forming units. Toward this end, compound **48** was dosed at 20, 40, 80, 160, and 320 mg/kg intraperitoneally, with linezolid (po, 20, 80, 320 mg/kg) and daptomycin (ip, 32 mg/kg) as positive controls. At the end of the experiment, animals that were administered vehicle in lieu of antibiotic had approximately 10^8 colony forming units in the thigh. Compound **48** prevented the increase in initial bacterial load at doses of 80–320 mg/kg at both 12 and 24 h. At 40 mg/kg, compound **48** was bacteriostatic only at the 12 h time point.

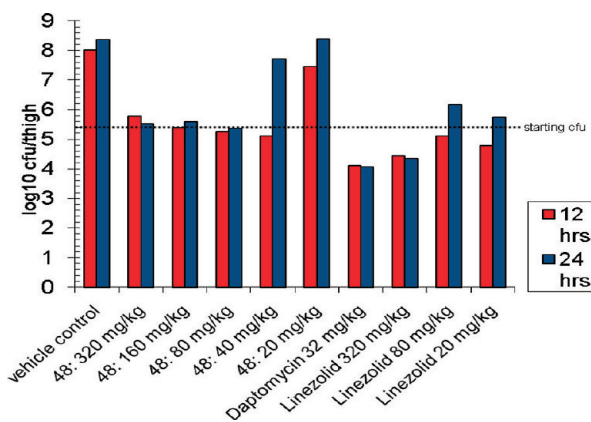


Figure 3. Bacteriostatic effect of **48** in a *S. aureus* thigh model of infection at 12 and 24 h.

In contrast, linezolid was bacteriostatic at 12 h at 80 mg/kg but had a slightly inferior effect compared to **48** at 24 h. Daptomycin proved superior to both **48** and linezolid, showing significant reduction at both 12 and 24 h at 32 mg/kg. These experiments were also performed with **58** and did not differ significantly.

DISCUSSION AND CONCLUSIONS

In summary, 4-aminothiazolyl analogues of the antibiotic natural product **1** were designed, synthesized, and evaluated for Gram positive bacterial growth inhibition. 4-Aminothiazole analogues with varying linker topologies, termini, and spacing between the macrocycle and the side chain terminus were evaluated for antibacterial activity. A trans-cycloalkylcarboxylic acid 4-aminothiazole side chain improved the antibacterial effect in vitro and in mouse sepsis and thigh models of infection. Cocrystallographic studies revealed the inhibitors' binding location and conformation in addition to important interactions between the cyclohexylcarboxylic acid functional motif and EF-Tu. In pharmacokinetic studies, **48** had low $V_{d,ss}$, low CL, and nonlinear exposure when dose was escalated and had minimal oral bioavailability. In a mouse thigh model of infection **48** proved bacteriostatic at doses greater than 80 mg/kg which was compared with the clinical standards of care (linezolid and daptomycin). On the basis of the superior antibacterial activity and the ionizable nature of their carboxylate side chains that facilitated formulation development,¹³ amide **48** and urethane **58** were selected for further preclinical profiling as development candidates.¹⁴ Taken together, these data supported further chemical scale-up, process optimization, and evaluation of **48** and **58** in rodent and nonrodent safety studies. Finally, the 4-aminothiazolyl-based chemical template described herein is a unique scaffold for antibacterial drug discovery. Indeed, in order to combat increasing clinical resistance to marketed antibiotics, the discovery of innovative chemical scaffolds that address underexploited antibacterial mechanisms of action remains a pressing need in infectious disease care. Thus, the biological activity exhibited by the cycloalkylcarboxylic acid class of thiopeptides is a significant and promising lead for antibiotic drug discovery. These development candidate identification efforts also impart further relevance to natural-product-based, industrial drug discovery. The details of these continued efforts will be the subject of additional correspondence.

EXPERIMENTAL SECTION

Compound Synthesis and Characterization. Synthetic procedures and compound characterization data are found in the Supporting Information. Compound purity was assessed by two distinct 20 min HPLC runs to confirm >95% purity.

MIC Assays. MIC assays were conducted according to the Clinical and Laboratory Standards Institute (CLSI): Wikler, M. A.; Cockerill, F. R.; Bush, K.; et al. *Methods for Dilution Antimicrobial Susceptibility Tests for Bacteria that Grow Aerobically, Approved Standard—Eighth Edition*; CLSI M07-A8; 2009; Vol. 29, No. 2; bacterial strains included *E. faecalis* (ATCC 29212), *E. faecium* (Prof. Chopra, University of Leeds, U.K., strain 7130724), *S. aureus* (MRSA from Prof. Willinger, isolated from a pharyngeal smear, AKHVienna A4.018), and *S. pyogenes* (ATCC BAA-595); Wikler, M. A.; Cockerill, F. R.; Bush, K.; et al. *Performance Standards for Antimicrobial Susceptibility Testing, Nineteenth Informational Supplement*; CLSI M100-S19, 2009; Vol. 29, No. 3.

In Vitro Transcription/Translation Assays. The *E. coli* S30 extract system for circular DNA (Promegacatalog no. L1020) was used per recommendation of the manufacturer with slight modifications. Briefly, 3.5 μ L of 286 ng/ μ L template DNA (pBESTluc) was mixed with 1.0 μ L each of 1 mM "methionineminus" and "cysteine minus" amino acid mixes, 8 μ L of S30 premix, 6 μ L of S30 extract, and 0.5 μ L of the test agents at 40 \times final concentration in a total volume of 20 μ L. The reaction mixtures were incubated for 2 h at 37 $^{\circ}$ C in a 384-well flat-bottom white plate (Corning, catalog no. 3704). The formation of luciferase was measured by adding equal volume (20 μ L) of Steady-Glo luciferase reagent (Promega catalog no. 27104), and emitted light was detected with a luminometer (Molecular Devices, LMaxII plate reader). Kirromycin and puromycin, which are known to be protein synthesis inhibitors, were used as positive controls. Ampicillin was used as a negative control. The rabbit reticulocyte TnT Quick coupled transcription/translation system (Promega catalog no. L1170) was used as recommended by the manufacturer except that the assay volumes were scaled down from 50 to 20 μ L. Briefly the assay components consisted of 16 μ L of TnT Quick mastermix, 3 μ L of pT7luc at 167 ng/ μ L, 0.5 μ L of methionine, and 0.5 μ L of the test compound at 40 \times final concentration in a final volume of 20 μ L. The reaction mixtures were incubated at 37 $^{\circ}$ C for 75 min. Luminescence was detected as described above.

Selection for Spontaneous, Single-Step Mutants. Multiple strains of *S. aureus*, *E. faecalis*, or *E. faecium* were streaked from glycerol stocks onto blood agar plates and incubated overnight at 37 $^{\circ}$ C. Duplicate sterile tubes containing either 5 mL Mueller Hinton or brain heart infusion broth were inoculated with three to five isolated colonies and incubated overnight with shaking at 37 $^{\circ}$ C. Saturated cultures were diluted $1/50$ in duplicate flasks containing 50 mL of fresh broth and incubated with shaking at 37 $^{\circ}$ C for 4.5 h for *S. aureus* or 7 h for enterococci. The culture densities were approximately 10¹⁰ cfu/mL. The duplicate cultures were concentrated 10-fold by centrifugation in 10 mL aliquots at 3500g for 20 min using a Sorvall Legend RT centrifuge. An amount of 1 mL of each 10-fold concentrated cell suspension was spread onto selection plates containing test agents. Selection plates were incubated for 48 h at 37 $^{\circ}$ C. Resistance frequency was defined as the number of colonies selected divided by the total cfu plated. Representative colonies were restreaked for isolated colonies on plates containing the selecting agent at 2 \times MIC against the isogenic parent. The restreaked cultures were suspended in Mueller Hinton or brain heart infusion broth + 20% glycerol and frozen at -80 $^{\circ}$ C.

Genetic Characterization of Mutants. PCR primers specific for *S. aureus* tufA, *E. faecalis* tuf, and *E. faecium* tufA and tufB were used to amplify tuf genes from representative single-step mutants and isogenic parental strains. Amplified fragments were sequenced at Agencourt (Beverly, MA), and sequences were aligned with ClustalW.

Mouse Systemic Infection Model. The studies conducted were approved by the Institutional Animal Care and Use Committee of the Novartis Institutes for BioMedical Research Inc., Cambridge, MA. Animals were maintained under controlled conditions with free access to food and water. Female CD1 mice (21–25 g, Charles

Table 7

parameter	48	58
	Data Collection (Highest Resolution Shell)	
resolution range (Å)	8.00–2.15 (2.28–2.15)	43–2.45 (2.60–2.45)
total observations	36 399	30 572
unique reflections	39 701	32 122
completeness (%)	88.6	94.8
I/σ	23.8 (8.0)	25.8 (4.0)
R_{sym}	0.098	
	Refinement	
$R_{\text{work}}/R_{\text{free}}$	0.211/0.273	0.224/0.298
no. protein atoms	5766	5996
no. heterogen atoms (Mg/GDP/compd)	168	170
no. solvent atoms	111	145
average B -factor (Å ²)	38.5	50.6
	Root Mean Squared Deviation from Ideal Value	
bond length (Å)	0.011	0.011
bond angle (deg)	1.4	1.2

RiverLaboratories, Wilmington, MA) were used for infections with *S. aureus* (ATCC 49951) and *E. faecalis* (NB04025, a clinical isolate from the Novartis bacterial collection that is resistant to erythromycin, tetracycline, and gentamicin, courtesy of Dr. B. Willinger, Vienna General Hospital, Austria). Lethal infections were induced by intraperitoneal injection of a freshly prepared bacterial suspension of 1×10^8 cfu/mouse in either 50% sterile rat fecal extract (*E. faecalis*) or 0.9% NaCl (*S. aureus*). The injected bacterial dose corresponded to 10–100 times the minimal lethal dose as determined from previous lethal dose titration studies. Therapy for *E. faecalis* infections was initiated immediately following the bacterial inoculation, while for *S. aureus* infections, therapy was initiated 1 and 5 h after inoculation. Compounds were administered via tail vein bolus injection at several dose levels to groups of six mice each. Following inoculation the mice were observed for 5 days. In addition, body temperature was monitored by electronic microtransponders (Bio Medic Data Systems, Inc., Seaford, DE) that were implanted in mice subcutaneously prior to infection. The 50% effective dose (ED_{50}), the dose providing protection to 50% of mice, and the 95% confidence limits (95% CI) were calculated from the survival data at day 5 by probit analysis using the program Systat (SPSS Inc.).

Mouse Thigh Infection Model. The studies conducted were approved by the Institutional Animal Care and Use Committee of the Novartis Institutes for BioMedical Research Inc., Cambridge, MA. Animals were maintained under controlled conditions with free access to food and water. Female CD1 mice (21–25 g, Charles River Laboratories, Wilmington, MA) were used for infections with *S. aureus* (ATCC 01001). Inoculum was prepared by adding 20 μ L from the ampule to 25 mL of Mueller Hinton + cations, then incubated with shaking for 16 h at 36 °C. The culture was diluted 1:50, and the OD_{600} was determined. The cfu/mL was determined for overnight culture and each subsequent dilution and was diluted 1:50 appropriately to achieve the target inoculum cfu/mL of 1.5×10^7 (7.5×10^5 cfu/thigh). Pretreatment (to induce neutropenia) included dosing 4 days prior to the study (150 mg/kg cyclophosphamide dosed intraperitoneally; 600 mg was dissolved in 20 mL saline to achieve 30 mg/mL; application volume of 0.5 mL/100g) and then 1 day prior to the study (100 mg/kg cyclophosphamide dosed intraperitoneally; 400 mg was dissolved in 20 mL saline to achieve 20 mg/mL; application volume of 0.5 mL/100 g). The left thigh was subsequently infected with 0.05 mL of inoculum (intramuscular injection). The animals (four per group) were then treated intraperitoneally with compound 48 at 320, 160, 80, 40, 20 mg/kg; treated with daptomycin (intraperitoneally) at 32 mg/kg; treated with linezolid (per os) at 80, 20 mg/kg; treated with vehicle (intraperitoneally). Colony forming units were then evaluated by excising the thigh muscle and storing on ice, homogenizing in 5 mL of 0.9% NaCl. Samples were serially diluted 1:10 (0.5 + 4.5 mL) in 0.9% NaCl,

and an amount of 100 μ L was pipetted onto blood agar plates for counting using the ProtoCOL system.

Solubility Measurements. An amount of 1–2 mg of compound was weighed into 1 mL glass tubes, and a fixed volume of each vehicle was added to yield approximately 20 mg/mL compound (48 or 58). After initial mixing using brief vortexing and sonication (5–10 min), samples were equilibrated by shaking for 24 h at room temperature. After equilibration, the vials were visually examined. If a clear solution was obtained, solubility was reported as $>X$ mg/mL (where X is the starting concentration in that sample) and the pH of this sample was recorded. Suspensions or solutions with visible particles were filtered through 0.22 μ m PVDF membrane filters. Their pH was recorded, and dissolved drug concentration was analyzed using a RP-HPLC assay.

Rat Pharmacokinetic Studies. Intravenous PK studies ($N = 2$ or 3) were performed with male Sprague–Dawley rats weighing 220–270 g and approximately 6–10 weeks old, which were obtained from Harlan Research Laboratories (South Easton, MA), each bearing dual implanted jugular vein cannula. The rats were fasted overnight before use and for 8 h after dosing. Blood samples were taken into K2EDTA coated tubes and then centrifuged to yield plasma sample for analysis by LC–MS/MS. Bioanalyses of rat plasma, from both in-life and protein binding experiments, were performed by LC–MS/MS using a system with the following configuration: Agilent liquid chromatograph (Santa Clara, CA), LEAP Technologies CTC-PAL autosampler (Carrboro, NC), and Applied Biosystems API 4000 mass spectrometer (Framingham, MA). LC was performed in gradient mode with reversed phase C18 columns (2.1 mm \times 30–50 mm \times 3.5–5 μ m particle size). Mobile phase A was 0.1% formic acid in water, and mobile phase B was 0.1% formic acid in acetonitrile. Gradients were run from 5% B to 95% B in \sim 3.5 min. Plasma samples were protein precipitated with acetonitrile containing glyburide as the internal standard (Sigma-Aldrich, St. Louis, MO).

Protein Binding. Protein binding was determined in triplicate using the rapid equilibrium dialysis device (Pierce Biotechnology, Rockford, IL) according to manufacturer specifications and protocol.

Crystallization and X-ray of Compound 48. To form the EF-Tu/48 complex, 10 mg/mL protein (227 μ M) *E. coli* EF-Tu protein in a buffer containing 50 mM Tris, pH 8, and 50 mM NaCl were incubated with 1 mM compound 1 for 1 h at 4 °C. The sample was centrifuged at 20000g to remove any resulting precipitant. Crystallization was carried out using 300 nL of the protein sample plus 300 nL of crystallization solution containing 0.1 M Bis-Tris, pH 6.5, 22% PEG 3350, 0.2 M ammonium acetate, using a sitting drop format and equilibrated against a reservoir of the crystallization solution. The crystals were flash frozen with liquid nitrogen after being stabilized in a cryobuffer containing 0.1 M Bis-Tris, pH 6.5, 22% PEG 3350, 0.2 M ammonium acetate, 20% ethylene glycol.

X-ray Data Collection. Initial data from a single crystal were collected on an ADSC Quantum 210 CCD detector using synchrotron radiation ($\lambda = 1 \text{ \AA}$) at the IMCA-CAT beamline 17-ID of the Argonne Photon Source. Data were collected using φ rotations of 0.5° , and 180° of total data were collected.

X-ray Data Processing, Structure Determination, and Refinement. Data were processed using the HKL2000 Suite, version 0.95. Data-processing statistics are shown in Table 7. Crystals were diffracted to 2.15 \AA resolution in the space group C222(1) with a unit cell of $a = 97.246 \text{ \AA}$, $b = 100.376 \text{ \AA}$, $c = 156.483 \text{ \AA}$, $\alpha = \beta = \gamma = 90^\circ$. Data collection statistics are shown in Table 7. The structure of the EF-Tu/GDP/48 complex was determined by molecular replacement as implemented in PHASER (20), using *E. coli* EF-Tu protein as a search model (1D8T). The resulting molecular replacement solution contained two EF-Tu/48 protein molecules in the asymmetric unit. Refinement was carried out with CNX (21) using a single round of rigid-body refinement, following several cycles of simulated annealing refinement, B-factor refinement, and model building with the COOT software package. Water molecules, GDP, and the Mg^{2+} ion were added prior to addition of the ligand 48. Refinement produced a final model with excellent geometry (rmsd bond length of 0.011 \AA , rmsd bond angle of 1.4°) and R_{work} and R_{free} of 21.1% and 27.3%, respectively.

Crystallization and X-ray of Compound 58. To form the EF-Tu/58 complex, 10 mg/mL protein ($227 \mu\text{M}$) *E. coli* EF-Tu protein in a buffer containing 50 mM Tris, pH 8, and 50 mM NaCl were incubated with 1 mM compound 1 for 1 h at 4°C . The sample was centrifuged at $20000g$ to remove any resulting precipitant. Crystallization was carried out using 300 nL of the protein sample plus 300 nL of crystallization solution containing 0.1 M Hepes, pH 7.5, 22% PEG 3350, 0.2 M MgCl_2 , using a sitting drop format and equilibrated against a reservoir of the crystallization solution. The crystals were flash frozen with liquid nitrogen after being stabilized in a cryobuffer containing 0.1 M Hepes, pH 7.5, 22% PEG 3350, 0.2 M MgCl_2 , 20% ethylene glycol.

X-ray Data Collection. Initial data from a single crystal were collected on an ADSC Quantum 210 CCD detector using synchrotron radiation ($\lambda = 1 \text{ \AA}$) at the IMCA-CAT beamline 17-ID of the Argonne Photon Source. Data were collected using φ rotations of 0.5° , and 180° of total data were collected.

X-ray Data Processing, Structure Determination, and Refinement. Data were processed using the HKL2000 Suite, version 0.95. Data-processing statistics are shown in Table 7. Crystals were diffracted to 2.45 \AA resolution in the space group P2(1)2(1)2(1) with a unit cell of $a = 80.372 \text{ \AA}$, $b = 82.216 \text{ \AA}$, $c = 129.9 \text{ \AA}$, $\alpha = \beta = \gamma = 90^\circ$. Data collection statistics are shown in Table 7. The structure of the EF-Tu/GDP/58 complex was determined by molecular replacement as implemented in PHASER, using *E. coli* EF-Tu protein as a search model (1D8T). The resulting molecular replacement solution contained two EF-Tu/58 protein molecules in the asymmetric unit. Refinement was carried out with CNX using a single round of rigid-body refinement, following several cycles of simulated annealing refinement, B-factor refinement, and model building with the COOT software package. Water molecules, GDP, and the Mg^{2+} ion were added prior to addition of the ligand. Refinement produced a final model with excellent geometry (rmsd bond length of 0.011 \AA , rmsd bond angle of 1.2°) and R_{work} and R_{free} of 22.4% and 29.8%, respectively.

■ ASSOCIATED CONTENT

● Supporting Information

Detailed synthetic procedures and compound characterization data. This material is available free of charge via the Internet at <http://pubs.acs.org>.

■ AUTHOR INFORMATION

Corresponding Author

*Telephone: (617) 871-7729. Fax: 617-871-4081. E-mail: matthew.lamarche@novartis.com.

■ ACKNOWLEDGMENTS

We thank Karl Gunderson and Bing Wang for their analytical support and the Natural Products Unit for their collaboration.

■ ABBREVIATIONS USED

MIC, minimum inhibitory concentration; EC_{50} , 50% effective dose; G+, Gram positive; MRSA, methicillin resistant *Staphylococcus aureus*; VRE, vancomycin resistant enterococci; *S. aureus*, *Staphylococcus aureus*; *E. faecalis*, *Enterococcus faecalis*; *E. faecium*, *Enterococcus faecium*; *S. pyogenes*, *Streptococcus pyogenes*; EF-Tu, elongation factor Tu

■ REFERENCES

- (1) Poulakou, G.; Giamarellou, H. Investigational Treatments for Postoperative Surgical Site Infections. *Expert Opin. Invest. Drugs* **2007**, *16* (2), 137–155.
- (2) (a) Selva, E.; Beretta, G.; Montanini, N.; Sandler, G. S.; Gastaldo, L.; Ferrari, P.; Lorenzetti, R.; Landini, P.; Ripamonti, F.; Goldstein, B. P.; Berti, M.; Montanaro, I.; Denaro, M. Antibiotic GE2270 A: A Novel Inhibitor of Protein Synthesis. *J. Antibiot.* **1991**, *44* (7), 693–701. (b) The structure was later corrected and verified: Tavecchia, P.; Gentili, P.; Kurz, M.; Sottani, C.; Bonfichi, R.; Selva, E.; Lociuro, S.; Restelli, E.; Ciabatti, R. Degradation Studies of MDL62,879 (GE220 A) and Revision of the Structure. *Tetrahedron* **1995**, *51* (16), 4867–4890. For acidic decomposition, see above.
- (3) (a) LaMarche, M. J.; Leeds, J. A.; Dzik-Fox, J.; Gunderson, K.; Krastel, P.; Memmert, K.; Patane, M. A.; Rann, E. M.; Schmitt, E.; Tiamfook, S.; Wang, B. 4-Aminothiazolyl Analogues of GE2270 A: Antibacterial Lead Finding. *J. Med. Chem.* **2011**, *54*, 2517–2521. (b) LaMarche, M. J.; Leeds, J. A.; Dzik-Fox, J.; Mullin, S.; Patane, M. A.; Rann, E. M.; Tiamfook, S. 4-Aminothiazolyl Analogues of GE2270 A: Design, Synthesis, and Evaluation of Imidazole Analogs. *Bioorg. Med. Chem. Lett.* **2011**, *21*, 3210–3215.
- (4) (a) Wikler, M. A.; Cockerill, F. R.; Bush, K. *Performance Standards for Antimicrobial Susceptibility Testing; Nineteenth Informational Supplement*; CLSI M100-S19; Clinical and Laboratory Standards Institute: Wayne, PA, 2009; Vol. 29, No. 3. (b) *Methods for Dilution Antimicrobial Susceptibility Tests for Bacteria that Grow Aerobically; Approved Standard—Eighth Edition*; CLSI M07-A8; Clinical and Laboratory Standards Institute: Wayne, PA, 2009; Vol. 29, No. 2.
- (5) The *tufA* gene encodes for the EF-Tu protein. The amino acid substitution G258D is located in domain 2 of the binding pocket of the thiopeptides. Zuurmond, A. M.; de Graaf, J. M.; Olsthoorn-Tieleman, L. N.; van Duyl, B. Y.; Morhle, V. G.; Jurnak, F.; Mesters, J. R.; Hilgenfeld, R.; Kraal, B. GE2270A-Resistant Mutations in Elongation Factor Tu Allow Productive Aminoacyl-tRNA Binding to EF-Tu-GTP-GE2270A Complexes. *J. Mol. Biol.* **2000**, *304*, 995–1005.
- (6) (a) Clough, J.; Chen, S.; Gordon, E. M.; Hackbarth, C.; Lam, S.; Trias, J.; White, R. J.; Candiani, G.; Donadio, S.; Romano, G.; Ciabatti, R.; Jacobs, J. W. Combinatorial Modification of Natural Products: Synthesis and In Vitro Analysis of Derivatives of Thiazole Peptide Antibiotic GE2270 A: A-Ring Modifications. *Bioorg. Med. Chem. Lett.* **2003**, *13*, 3409–3414. (b) Malabarba, M.; Cavaleri, M.; Mosconi, G.; Jabes, D.; Romano, G. Use of Amide Derivative of GE2270 Factor A3 for the Treatment of Acne. Patent WO03105881, 2003.
- (7) Chemical stability was measured by incubation of compound at pH 1, 4, 7 at room temperature, 50°C , and 80°C for 1 week. Degradation was measured by LC/MS and quantified by AUC.
- (8) (a) Zubay, G. In Vitro Synthesis of Protein in Microbial Systems. *Annu. Rev. Genet.* **1973**, *7*, 267–287. (b) Zubay, G. Isolation and Properties of CAP, the Catabolite Gene Activator. *Methods Enzymol.* **1980**, *65*, 856–877.
- (9) Frimodt-Møller, N.; Knudsen, J. D.; Espersen, F. *Handbook of Animal Models of Infection*; Zak, O., Sande, M. A., Eds.; Academic Press: San Diego, CA, 1999; pp 127–136.

(10) The coordinates for the cocrystal structures for **48** and **58** and EF-Tu were deposited at the Protein Data Bank under codes 3U6B and 3U6K, respectively.

(11) Heffron, S. E.; Jurnak, F. Structure of an EF-Tu Complex with a Thiazolyl Peptide Antibiotic Determined at 2.35 Å Resolution: Atomic Basis for GE2270 A Inhibition of EF-Tu. *Biochemistry* **2000**, *39*, 37–45.

(12) Gudmundsson, S., Erlendsdóttir, H., Zak O., Sande, M. A., Eds. *Handbook of Animal Models of Infection*; Academic Press: San Diego, CA, 1999; pp 137–144. The mouse thigh model of infection: mice, CD1:ICR (44); *Staphylococcus aureus* strain NB 01001; target inoculum cfu/mL of 1.5×10^7 (7.5×10^5 cfu/thigh); infection, 0.05 mL intramuscular injection in the left thigh; cyclophosphamide administered on day 4 and day 1; infection, 2 h, all mice; treatment at 0 h and evaluation at 12 or 24 h; for evaluation, excise thigh muscles and store on ice; homogenize, serially dilute in 0.9% NaCl, and pipette 100 μ L onto blood agar plates for counting using ProtoCOL system.

(13) Carboxylate containing compounds could generally be formulated with 5% PEG. **48** and **58** were formulated up to 20 mg/mL using 5% PEG300, 0.1 M NaOH, and pH 7.4 buffer.

(14) Leeds, J. A.; LaMarche, M. J.; Brewer, J. T.; Bushell, S. M.; Deng, G.; Dewhurst, J. M.; Dzink-Fox, J.; Gangl, E.; Jain, A.; Lee, L.; Lilly, M.; Manni, K.; Mullin, S.; Neckermann, G.; Osborne, C.; Palestrant, D.; Patane, M.A.; Raimondi, A.; Ranjitkar, S.; Rann, E. M.; Sachdeva, M.; Shao, J.; Tiamfook, S.; Whitehead, L.; Yu, D. In Vitro and in Vivo Activities of Novel, Semi-Synthetic Thiopeptide Inhibitors of Bacterial Elongation Factor Tu. *Antimicrob. Agents Chemother.* [Online early access]. DOI: 10.1128/AAC.00582-11. Published Online: Aug 8, 2011.

■ NOTE ADDED AFTER ASAP PUBLICATION

This paper was published on the Web on November 1, 2011 without the author's corrections. The correct version was reposted on November 3, 2011.